2026 IEEE/SICE International Symposium on System Integration (SII)
January 11-14, 2026. Cancún, México

Development of Hand Skeleton with Jamming Transition for Improved Object Grasp Retention Force and Stable Leader–Follower Teleoperation Grasping in Soft Robotic Hand*

Yusuke Yamashita[1] Yuki Funabora[1] and Shinji Doki[1]

Abstract— **In this paper, we present a soft robotic hand structure capable of enhancing object grasp retention force and achieving stable object grasping under teleoperation without haptic feedback. The soft robotic hand consists of a hand skeleton equipped with a soft glove device actuated by extra-thin McKibben artificial muscles. In this paper, a particle layer was integrated into the hand skeleton, and the jamming transition was implemented by applying a vacuum to this particle layer. The jamming transition increases the driving force required to actuate the fingers of the hand skeleton, thereby improving the object grasp retention force of the soft robotic hand. Finally, as a demonstration, teleoperation was performed using leader–follower control without haptic feedback. The results show that activating the jamming transition after grasping an object enables the hand to maintain a stable grasp regardless of the leader's posture.**

I. Introduction

Recently, increasing attention has been paid to robotic hands that mimic the human hand [1] [2]. Such robotic hands have five fingers, similar to the human hand, and are capable of multi-degree-of-freedom actuation. Therefore, they are expected to be utilized in applications such as teleoperation, where the movements of a human hand are transmitted to a remote location [3] [4]. Robotic hands used for teleoperation are generally hard robotic hands equipped with motors or exoskeletons, but due to their rigidity, the range of objects that can be grasped and manipulated is limited. Consequently, in recent years, soft robotic hands actuated by soft actuators have been developed [5] [6]. Soft robotic hands have the advantages of flexibility and light weight, making them well suited for handling fragile objects and for safe contact with humans [7]. However, because soft robotic hands have high backdrivability, they exhibit low output force, resulting in small object grasping forces [8]. Therefore, to improve the practicality of soft robotic hands, it is necessary to enhance their object grasping force.

Our research group has also been conducting studies on a newly designed soft robotic hand structure [9].This structure consists of a soft glove device driven by soft actuators and incorporating a hand skeleton inside. By altering the characteristics of the soft glove device and the hand skeleton according to the application, it is possible to change the performance of the soft robotic hand, providing high adaptability. In previous work [9], grasping tests for various objects were conducted, and while the hand was able to grasp objects such as balls and plastic bottles, it was found to share the same limitation as general soft robotic hands in that it could not grasp heavy objects effectively. In this paper, we aim to improve the object grasp retention force by modifying the structure of the hand skeleton.

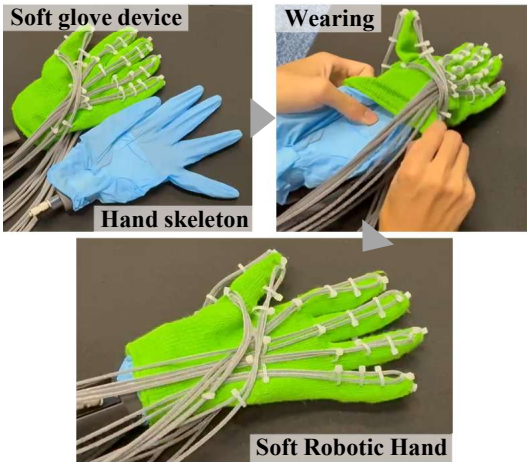

Fig. 1: Structure of Soft Robotic Hand : Composed by mounting a soft glove device onto a hand skeleton

As related work, Mizushima et al. developed a robotic hand equipped with a jamming transition mechanism [10]. This robotic hand used a tendon-driven joint actuation mechanism and incorporated a layer of particles in its outer shell. By applying a vacuum to the particle layer, a jamming transition was induced, which fixed the joints and increased the grasp retention force of the robotic hand.

In this paper, we develop a hand skeleton with a jamming transition mechanism as the internal structure of our soft robotic hand, aiming to improve its object grasp retention force. Furthermore, in previous studies, the soft glove device was equipped with soft actuators on only four fingers; in this work, we additionally equip the thumb with a soft actuator to enable five-finger actuation of the soft robotic hand.

In many teleoperation systems, bilateral control is employed to provide force feedback, enabling the leader to perceive the force exerted during object grasping and thereby maintain the grasp [4] [11]. However, robotic hand–glove systems employing bilateral control are complex, and constructing such systems is not straightforward. Therefore,

*This work was supported by JSPS KAKENHI Grant Number JP23H03475.

[1]Graduate School of Engineering, Nagoya University, Nagoya, Japan yamashita.yusuke.f2@s.mail.nagoya-u.ac.jp

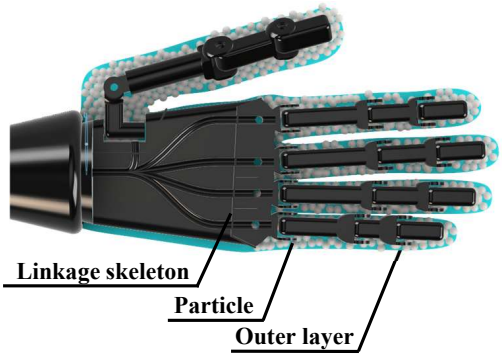

Fig. 2: Structure of Hand Skeleton

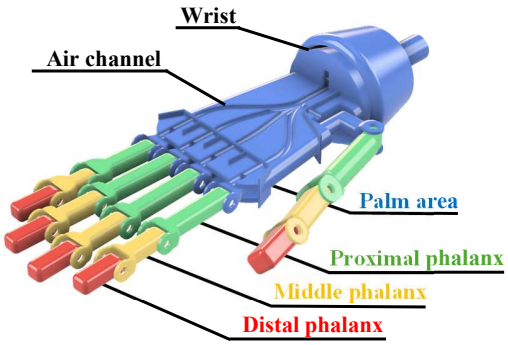

Fig. 3: Linkage skeleton

in this paper, we construct a system that can maintain a stable grasp even with a simple configuration such as leader–follower control without force feedback, by utilizing the jamming transition mechanism.

II. Soft Robotic Hand

The soft robotic hand has a two-layer structure, consisting of a soft glove device mounted on the outer surface of the hand skeleton (Fig. 1). The actuators of the soft glove device determine the actuation direction and actuation characteristics of the fingers of the soft robotic hand, while the link structure of the hand skeleton determines the link configuration of the soft robotic hand. In this paper, the hand skeleton is equipped with a jamming transition mechanism to improve the grasp retention force of the soft robotic hand. This section describes the composition of the soft robotic hand in the order of the hand skeleton, the jamming transition mechanism, the soft glove device, and the drive system.

A. Hand Skeleton

The model of the hand skeleton used in this study is shown in Fig. 2. The hand skeleton consists of three layers: a linkage skeleton, particles, and an outer layer. The particles are described in the next section on Jamming Transition.

The model of the linkage skeleton is shown in Fig. 3. The linkage skeleton consists of four parts: the palm area, the proximal phalanx, the middle phalanx, and the distal phalanx, similar to the human hand. Each joint is connected via a hinge joint, allowing frictionless motion with a range of motion equivalent to that of a human finger. The palm area contains an air channel, which enables the evacuation of air from each finger when applying a vacuum. In addition, a gasket is installed at the wrist of the palm area, enabling complete sealing between the linkage skeleton and the outer layer.

The linkage skeleton was fabricated using a 3D printer (Markforged Mark Two) with ONIX material, a composite of carbon fiber and nylon. The linkage skeleton weighs 107 g, with a length of 210 mm from the wrist to the fingertip and a width of 100 mm, dimensions comparable to those of an average human hand.

For the outer layer, a rubber glove (NO882-LL, MiSUMi) was used. The rubber glove has a thickness of 0.075 mm, an overall length of 240 mm, and a mass of 5 g, and can be used under vacuum conditions for the jamming transition without tearing.

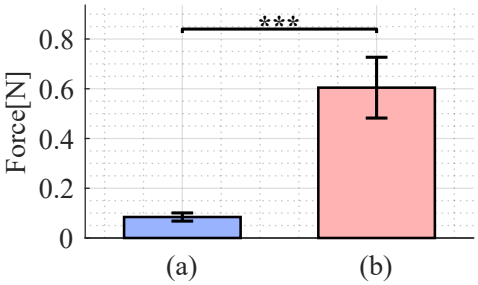

Fig. 4: Driving force: (a) without activating the jamming transition (n : 5, SD : 0.0164), (b) with activating the jamming transition (n : 5, SD : 0.1222)

B. Jamming Transition

For the particles used in the jamming transition, polystyrene foam balls with a diameter of 0.5 mm (B003DT1V9E) were employed. As shown in Fig. 2, the particles were packed between the finger sections of the linkage skeleton and the outer layer, and a total of 7 g of polystyrene foam balls was used.

The particles must not interfere with finger actuation when the soft robotic hand is driven, but must fix the posture during object grasping by means of the jamming transition, i.e., restrict finger actuation. This is achieved by altering the driving force required for finger actuation through the activation of the jamming transition. Therefore, the driving force of the fingers in the hand skeleton was measured both without and with activating the jamming transition. The driving force of a finger was measured by fixing the palm area of the hand skeleton so that it faced sideways and measuring the force required for the fingertip of the middle finger to move 7 mm toward the back side of the hand from the state shown in Fig. 2. The results are shown in Fig. 4. (a) shows the driving force of the middle finger without activating the jamming transition, while (b) shows the driving force with activating the jamming transition (*** : $p < 0.001$). The results indicate that activating the jamming transition increases the driving force by approximately six

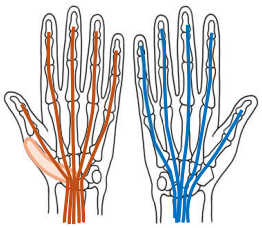

Fig. 5: Human musculoskeletal arrangement

Fig. 6: Soft Glove Device

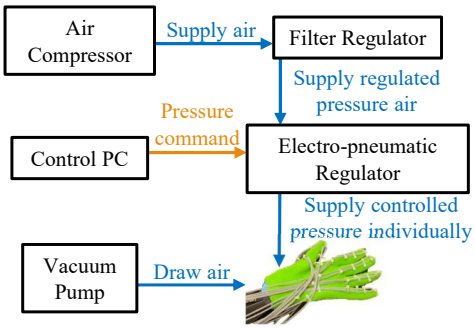

Fig. 7: Drive System

times, and a statistically significant difference was observed compared to the condition without activation. In addition, the driving force without activating the jamming transition was approximately 0.1 N, which does not impede finger actuation. From the above, it was confirmed that the particles used possess the potential to meet the specified requirements.

C. Soft Glove Device

The soft glove device was developed with the aim of inducing flexion and extension motions of the four fingers, as well as flexion, extension, palmar adduction, and palmar abduction motions of the thumb.

The musculoskeletal structures responsible for inducing these motions in an actual human hand are shown in Fig. 5. Finger flexion is induced by the flexor muscles, shown in red in Fig. 5, which extend from the center of the wrist to the fingertips [12]. Similarly, finger extension is induced by the extensor muscles, shown in blue in Fig. 5, which also extend from the center of the wrist to the fingertips [12]. Palmar adduction of the thumb is induced by the opponens pollicis muscle, shown in orange in Fig. 5, which extends from the center of the wrist to the MP joint of the thumb [12].

In this paper, as in previous studies [13], the actuator arrangement of the soft glove device was determined based on the musculoskeletal structure of the human hand. The soft glove device fabricated based on this arrangement is shown in Fig. 6.

In this soft glove device, the artificial muscles for flexion and extension actuate in opposition to each other. This opposition relationship follows that used in previous studies [13].

D. Drive System

The drive system of the soft robotic hand is shown in Fig. 7. The drive system consists of five components and has two functions: independently controlling the artificial muscles that drive each finger, and creating a vacuum inside the outer layer of the hand skeleton. The components are as follows. Air Compressor (SOL-1030, PAOCK): Supplies pneumatic pressure, Filter Regulator: Supplies constant pneumatic pressure, Control PC: Inputs the target pneumatic pressure to the electro-pneumatic regulators, Electro-pneumatic Regulators (CRCB-0135W/0136W, KOGANEI): Control the applied pneumatic pressure every 50 ms according to the target pneumatic pressure, Vacuum pump (DPV-ATAD, KOGANEI): Generates negative pneumatic pressure and evacuates the air inside the outer layer of the hand skeleton.

III. Investigation of the Effects of the Jamming Transition

In this section, the effects of the jamming transition on the grasp retention force and driving characteristics of the soft robotic hand are investigated.

A. Effects on Grasp Retention Force

The effect of activating the jamming transition on the grasp retention force of the soft robotic hand was investigated by comparing the grasp retention force with and without activation of the jamming transition. The experimental procedure is as follows:

(1) Fix the soft robotic hand with the palm facing downward.
(2) Press an object (a pen) tied with a string to a force sensor (six-axis force sensor, Leptrino) against the palm.
(3) Apply pneumatic pressure of 400 kPa to the artificial muscles involved in object grasping to grasp the object.
(4) Without activating / with activating the jamming transition.
(5) Pull the force sensor in the direction of gravity.
(6) Measure the maximum exerted force until the object is released from the soft robotic hand.
(7) Repeat steps (1) to (6) ten times for both without and with activating the jamming transition.

Results and Discussion: The results are shown in Fig. 8. (a) shows the grasp retention force without activating the jamming transition, and (b) shows the grasp retention force with activating the jamming transition (***: $p < 0.001$). The results indicate that the grasp retention force was approximately 3.4 N without activating the jamming transition and approximately 5.2 N with activating the jamming transition, and a t-test confirmed that there was a statistically significant difference between the two conditions. This result is due to the increased finger driving force shown in Section II-D, where activating the jamming transition restricted posture changes from external forces during grasping.

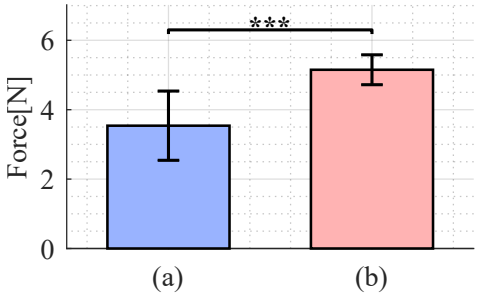

Fig. 8: Grasp retention force: (a) without activating the jamming transition (n : 11, SD : 0.9466), (b) with activating the jamming transition (n : 11, SD : 0.4086)

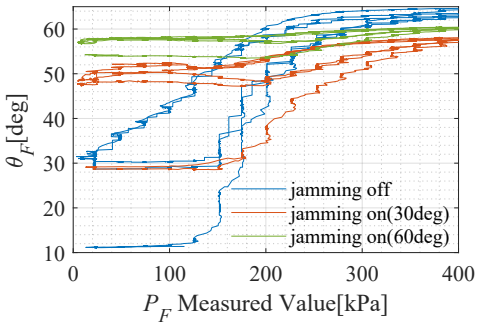

Fig. 9: Driving characteristics: (blue line) without activating the jamming transition, (red line) activating at 30°, (green line) activating at 60°

B. Effects on Driving Characteristics

Next, the effect of the jamming transition on the driving characteristics of the fingers was investigated. The experimental procedure is as follows:

(1) Fix the soft robotic hand with the palm facing downward.
(2) Without activating / activating the jamming transition at a 30° posture / activating the jamming transition at a 60° posture.
(3) Apply pneumatic pressure(P_F) to the artificial muscle that drives the index finger from 0 to 400 kPa (in increments of 25 kPa, then decreasing in increments of 25 kPa after reaching 400 kPa).
(4) Repeat step (3) three times.
(5) Measure the flexion angle at the MP joint(θ_F) using a motion capture system with seven cameras (OptiTrack).

Results and Discussion: The results are shown in Fig. 9. The blue line represents the driving characteristics of the finger without activating the jamming transition, the red line represents those when activating the jamming transition at a 30° posture, and the green line represents those when activating the jamming transition at a 60° posture. The results confirm that activating the jamming transition restricts finger actuation. In particular, when the jamming transition was activated at a 60° posture, almost no change in finger posture occurred, and the angle remained constant. Similarly, when activated at a 30° posture, the restriction of finger actuation was also observed; however, instead of being restricted exactly at 30°, the finger flexed to approximately 50° before the actuation was restricted.

This behavior is considered to be due to the torque applied to the MP joint. When the jamming transition was activated at 30°, all finger joints were almost fully extended, and the distance from the fingertip—where the artificial muscle force is applied—to the MP joint was long, resulting in a large torque being applied to the MP joint. In contrast, when the jamming transition was activated at 60°, all finger joints were almost fully flexed, and the distance from the fingertip to the MP joint was short, resulting in a smaller torque applied to the MP joint. Consequently, in the angular range where the torque applied by the artificial muscles exceeds the driving torque of the finger, the finger can still be actuated even when the jamming transition is activated, whereas in the angular range where the applied torque falls below the driving torque, the finger actuation is restricted.

From the above, it was confirmed that this soft robotic hand can impede finger actuation by activating the jamming transition in an angular range used for object grasping. Therefore, under leader–follower control in teleoperation, the hand can maintain a grasp without finger actuation even if the commanded finger angle changes.

IV. Object Grasping Experiments

Next, the functionality of the soft robotic hand was evaluated by having it grasp multiple types of objects. The objects to be grasped by the soft robotic hand were a sponge ball, a rubber baseball, a hammer, a screwdriver, a cube, and aluminum frames (200 mm and 330 mm) — seven objects in total (Fig. 10(a)). The parameters of each object are shown in Fig. 10(b). The experimental procedure is as follows:

(1) Fix the soft robotic hand with the palm facing downward.
(2) Press the object to be grasped against the palm.
(3) Apply a pneumatic pressure of 400 kPa to the artificial muscles involved in object grasping to grasp the object.
(4) Without activating / with activating the jamming transition.
(5) After grasping the object, wait for 5 s and evaluate whether the grasp was maintained.
(6) For each object, evaluate both without and with activating the jamming transition five times each.

Results and Discussion: The results are shown in Fig. 10(c), (d), and (e). The numbers on each label indicate the number of successful grasps under each condition.

From Fig. 10(c), it was confirmed that the sponge ball, the 200 mm frame, and the screwdriver were stably grasped even without activating the jamming transition. These objects are lightweight and have a weight lower than the grasp retention force without the jamming transition, as shown in Section III-A. Furthermore, both the sponge ball and the screwdriver have compliant grasping surfaces, which deform to fit the shape of the grasping region, making them easier to grasp.

As shown in Fig. 10(d), the 330 mm aluminum frame and the hammer could not be grasped without activating the

(a) Objects

Object	L×H×W[mm]	Mass[g]
Sponge ball	70×70×70	14
Soft baseball	72×72×72	137
Cube	75×75×75	137
Hammer	308×30×108	430
Screwdriver	196×36×36	127
Frame(200mm)	200×30×30	154
Frame(330mm)	330×30×30	275

(b) Object's parameters

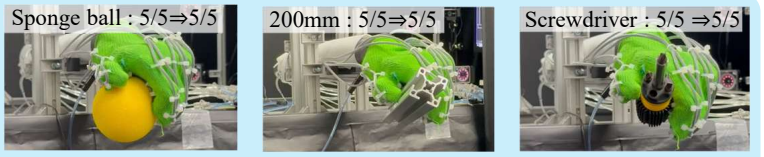

(c) Graspable objects under both conditions

(d) Graspable objects with significant change due to jamming transition

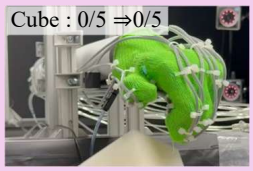

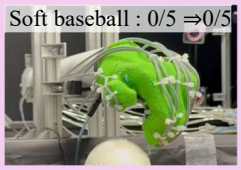

(e) Ungraspable objects under both conditions

Fig. 10: Object grasping experiment

jamming transition, but could be grasped when the jamming transition was activated. The hammer's weight was between the grasp retention force without and with the jamming transition. It is considered that the posture change of the fingers caused by the force exerted by the hammer on the fingers was restricted by activating the jamming transition, enabling the grasp. On the other hand, the frame (330 mm) had smooth sides with low friction, and there existed a threshold force—smaller than the grasp retention force shown in Section III-A—at which it could only be grasped when the jamming transition was activated. As a result, it could not be grasped without activating the jamming transition but could be grasped with activation.

Finally, As shown in Fig. 10(e), the cube and the rubber baseball could not be grasped. This is considered to be due to their size and rigidity. The cube exceeded the grasping range of the soft robotic hand and thus could not be grasped. Although the rubber baseball was similar in size to the sponge ball, its higher rigidity caused it to be deflected by the thumb and four fingers during grasping, preventing a successful grasp.

V. Demonstration

Finally, a demonstration was conducted to evaluate the effect of the jamming transition on object grasping under leader–follower control.

Leader-follower control

Leader–follower control used for teleoperation is described as follows. Based on the finger angles of the leader, which is the human operator, the finger angles of the follower, which is the soft robotic hand, are controlled. The finger angles of the leader are measured using a motion sensor(Leap Motion Controller 2, Ultraleap Ltd.). The measured angles are input to the control PC. Then, through empirically determined feedforward control, the angles are converted into applied pneumatic pressures, which are then input to the soft robotic hand. This enables posture control of the soft robotic hand in a remote environment.

Teleoperation

The teleoperation demonstration is shown in Fig. 11. The teleoperation procedure was carried out as follows:

(1) The leader places the left hand above the motion sensor (Fig. 11(a)).
(2) An experiment assistant presses an object (a screwdriver) against the palm of the soft robotic hand (Fig. 11(b)).
(3) When the object contacts the palm of the soft robotic hand, the leader moves the hand to grasp the object (Fig. 11(c)).
(4) After the soft robotic hand grasps the object, the leader activates the jamming transition (Fig. 11(c)).
(5) The leader relaxes the posture of the hand or shakes it in various directions (forward, backward, left, and right) to change the grasping posture (Figs. 11(d), (e)).
(6) The leader then opens the hand, deactivates the jamming transition, and releases the object (Fig. 11(f)).

As shown in Figs. 11(d) and 11(e), even when the leader's hand relaxed from the grasping posture or when posture

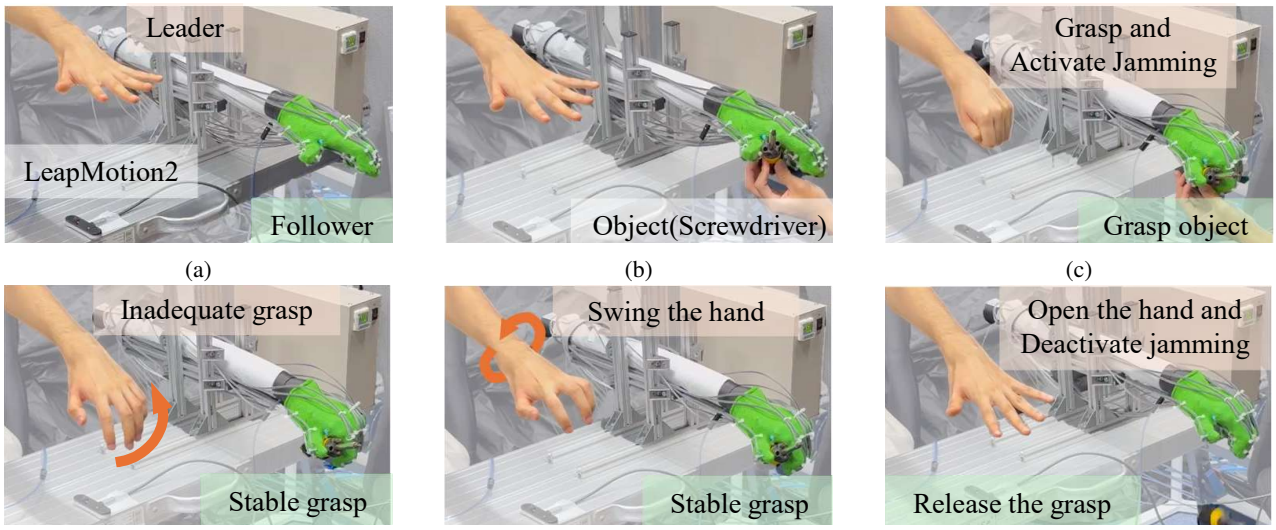

(a) (b) (c)

(d) (e) (f)

Fig. 11: Demonstration of teleoperation using leader–follower control

changes occurred due to excessive arm movement, the grasp was maintained. This confirms that stable object grasping can be achieved remotely, even with a simple system without force feedback.

VI. Conclusion

In this paper, a five-finger soft robotic hand was developed, consisting of a soft glove device mounted on a hand skeleton capable of activating the jamming transition. The hand skeleton of the soft robotic hand consists of a linkage skeleton, particles, and an outer layer. By applying a vacuum to the inside of the outer layer, a jamming transition occurs through the particles, which increases the driving force of the hand skeleton. With this structure, the soft robotic hand increased its grasp retention force by approximately 53% and expanded the range of objects it could grasp. The soft glove device of the soft robotic hand can induce flexion and extension motions of all five fingers. Furthermore, the drive system allows independent control of each finger posture. This structure enables the hand to mimic the posture of a human hand, and, as demonstrated in the experiments, it can be used for teleoperation.

In the demonstration, a leader–follower control system without force feedback was implemented, and teleoperation was performed. It was shown that, by activating the jamming transition after grasping an object, the grasp could be maintained without force feedback, demonstrating that stable grasping is possible even with a simple system.

Future work will aim to increase the range of motion of the soft robotic hand to enable the grasping of a wider variety of objects.

References

[1] S. K. Sampath, N. Wang, H. Wu, and C. Yang, "Review on human-like robot manipulation using dexterous hands." *Cogn. Comput. Syst.*, vol. 5, no. 1, pp. 14–29, 2023.

[2] S. A. Pertuz, C. H. Llanos, and D. M. Muñoz, "Development of a robotic hand using bioinspired optimization for mechanical and control design: Unb-hand," *IEEE Access*, vol. 9, pp. 61 010–61 023, 2021.

[3] Y. Qin, W. Yang, B. Huang, K. Van Wyk, H. Su, X. Wang, Y.-W. Chao, and D. Fox, "Anyteleop: A general vision-based dexterous robot arm-hand teleoperation system," *arXiv preprint arXiv:2307.04577*, 2023.

[4] D. Leonardis, M. Gabardi, S. Marcheschi, M. Barsotti, F. Porcini, D. Chiaradia, and A. Frisoli, "Hand teleoperation with combined kinaesthetic and tactile feedback: A full upper limb exoskeleton interface enhanced by tactile linear actuators," *Robotics*, vol. 13, no. 8, p. 119, 2024.

[5] M. Li, Y. Zhuo, J. Chen, B. He, G. Xu, J. Xie, X. Zhao, and W. Yao, "Design and performance characterization of a soft robot hand with fingertip haptic feedback for teleoperation," *Advanced Robotics*, vol. 34, no. 23, pp. 1491–1505, 2020.

[6] H. Wang, F. J. Abu-Dakka, T. N. Le, V. Kyrki, and H. Xu, "A novel soft robotic hand design with human-inspired soft palm: Achieving a great diversity of grasps," *IEEE Robotics & Automation Magazine*, vol. 28, no. 2, pp. 37–49, 2021.

[7] H. Banerjee, Z. T. H. Tse, and H. Ren, "Soft robotics with compliance and adaptation for biomedical applications and forthcoming challenges," *Int. J. Robot. Autom*, vol. 33, no. 1, pp. 68–80, 2018.

[8] S. Alves, M. Babcinschi, A. Silva, D. Neto, D. Fonseca, and P. Neto, "Integrated design fabrication and control of a bioinspired multimaterial soft robotic hand," *Cyborg and Bionic Systems*, vol. 4, p. 0051, 2023.

[9] Y. Yamashita, Y. Funabora, and S. Doki, "Research of the influence of skeletal structure on grasping performance to realize robotic hand consisting of hand skeleton and glove device," in *The 25th SICE System Integration Division Annual Conference (SI2024)*. The Society of Instrument and Control Engineers (SICE), 2024, pp. 1730–1731, [in Japanese].

[10] K. Mizushima, T. Oku, Y. Suzuki, T. Tsuji, and T. Watanabe, "Multi-fingered robotic hand based on hybrid mechanism of tendon-driven and jamming transition," in *2018 IEEE International Conference on Soft Robotics (RoboSoft)*. IEEE, 2018, pp. 376–381.

[11] P. Hu, X. Huang, Y. Wang, H. Li, and Z. Jiang, "A novel hand teleoperation method with force and vibrotactile feedback based on dynamic compliant primitives controller," *Biomimetics*, vol. 10, no. 4, p. 194, 2025.

[12] D. A. Neumann, "Kinesiology of the musculoskeletal system: Foundations for rehabilitation, 2e," *St. Louis, MO: Elsevier*, 2010.

[13] Y. Yamashita, Y. Funabora, and S. Doki, "Prototype of soft glove device for inducing finger movement in flexion-extension and adduction-abduction directions," in *2025 SICE Festival with Annual Conference (SICE FES)*. IEEE, 2025, pp. 663–668.